Spring 5-1-2019

Quantifying Expression of Interneuron Subtype Markers for Dlx-2 Transfected NG2 Cells

Timothy Nolan
timothy.nolan@uconn.edu

Quantifying Expression of Interneuron Subtype Markers for Dlx-2 Transfected NG2 Cells

Timothy Nolan
Undergraduate Honors Thesis
May 2019

Akiko Nishiyama Laboratory
Department of Physiology and Neurobiology
University of Connecticut

Table of Contents

Abstract

Neurons are a post-mitotic cell population, and therefore, they are not able to regenerate in vivo after a traumatic injury. Because inhibitory GABAergic interneurons and oligodendrocyte precursor cells (OPCs) are derived from the same precursor, recent studies have focused on transforming these OPCs into GABAergic neurons. However, there are different types of GABAergic interneurons that have different electrophysiological responses, which can lead to functional differences. The Nishiyama laboratory had already used a key gene in GABAergic interneuron and OPC differentiation, Distal-less homeobox 2 (Dlx-2), to transfect OPCs; early electrophysiology tests showed most of these transfected cells behaved like immature neurons, but some behaved how fast-spiking parvalbumin-containing GABAergic neurons would. To further clarify what type of GABAergic interneurons our Dlx-2 transfected cells are becoming, I chose fourteen genes to quantify and compare, utilizing reverse-transcriptase polymerase chain reactions (qRT-PCR). After designing and optimizing primer pairs to target these genes, five replicates of transfected cells were tested; results were analyzed using both the $2^{-\Delta\Delta CT}$ method and by evaluating raw cycle thresholds for each gene. Gad67, the gene responsible for producing GABA, was significantly more expressed in the Dlx-2-transfected samples, showing that these cells are differentiating into GABAergic interneurons. Although a few genes linked to the parvalbumin- and somatostatin-containing types of GABAergic interneurons were significantly more expressed in the Dlx-2-transfected samples, most genes were not significantly changed, suggesting that these cells are either expressing a mixed phenotype or are not developed enough at this time point to clearly show a subtype.

Introduction

The natural response of the adult cortical tissue to injury is not neurogenesis to replace the damaged neurons, but rather a glial response of migrating to the site of injury and inhibiting neurogenesis and further immune cell responses [1,2,3]. As a part of this response, certain central nervous system cell populations that are still mitotically active proliferate to enhance their response. Oligodendrocyte precursor cells (OPCs) are considered a fourth major glial cell type, making up 2-8% of glial cells in the brain; since these are ubiquitous, these are able to divide and differentiate into oligodendrocytes all throughout the brain [4]. OPCs are often characterized by their expression of the transmembrane proteoglycan NG2 [5,6] and the alpha receptor of platelet-derived growth factor (PDGFRa) [7]. NG2 is a neurexin, helping to strengthen synapses with nearby axons [8] and direct cell migration in development [9].

OPCs share the same progenitor cells with GABAergic interneurons, which are neurons that synapse onto other neurons and express the inhibitory neurotransmitter Gamma-aminobutyric acid (GABA), and the regulation of a few specific genes regulates which fate the progenitor cell will follow. These neural progenitor cells, or NPCs, originate in the ganglionic eminences [10] and start expressing the basic helix-loop-helix transcription factor Olig2 at E8.5 [11]; the subpopulation that express PDGFRa, starting at E13.5, are fully committed to becoming OPCs once they start expressing NG2, first seen at E15 [12,13]. NG2 is only expressed after the high-mobility-group transcription factors Sox9 and Sox10 are expressed alongside Olig2; both Sox10 and Olig2 bind to an enhancer for NG2, increasing its expression [14].

The Dlx homeodomain transcription factor family is a key regulator in NPC development during embryogenesis. By E12, NPCs in the lateral and medial ganglionic eminences are significantly expressing both Dlx-1 and Dlx-2, which will then stimulate expression of related transcription factors Dlx-5 and Dlx-6 [15]. Furthermore, the expression of transcription factors Dlx-1 and Dlx-2 has a negative correlation with the expression of the basic helix-loop-helix Ascl1 (formerly called Mash1), which actually has a binding site on the intergenic region between Dlx-1 and Dlx-2. Knocking out Ascl1 leads to increases in Dlx-1 and Dlx-2 expression and a decrease in OPC production from NPCs, whereas knocking out Dlx-1 and Dlx-2 leads to increased Ascl1 expression and OPC formation [16]. These findings suggest that Dlx-1 and Dlx-2 are directly related to the regulation of NPC differentiation and fate determination. In addition, when the Dlx-2 is knocked out, GABAergic interneuron differentiation can be impaired both in vivo and in vitro [17]; these mutations have also been shown to decrease the expression of Dlx5 and Dlx6[18]. Knocking out either the Dlx-1 or Dlx-2 gene also can impair neuronal migration in the striatum [19], and improper development of these GABAergic interneurons has been proposed to cause an imbalance leading to over-excitation in the cortex, and is potentially linked to Autism [20] . Because of its role in regulating NPC's differentiation into either GABAergic interneurons or OPCs, and the major neurodevelopmental defects associated when this gene is knocked out, Dlx-2 is an ideal gene to clone to induce oligodendrocyte precursor cells to follow a GABAergic interneuron fate.

These NG2 cells are known to differentiate into oligodendrocytes, but they are primarily committed to the oligodendrocyte lineage by the time of birth in vivo. In vitro, the potential for NG2 cells to de-differentiate into a multipotential neural stem cell has been shown under rare circumstance when they are cultured with appropriate mixes of extracellular signals or transcription factors [21]. Some cell culture studies showing isolated OPCs can become oligodendrocyte-type-2 astrocyte (O2A) progenitor cells, which could then differentiate into either astrocytes or oligodendrocytes; there are no identified in vivo analogs to these O2A progenitor cells, suggesting this finding may just be an artifact [7]. In vivo studies involving central nervous system lesions show these NG2 cells accumulate near the lesion, can contribute to the glial scarring, and can potentially differentiate into astrocytes or oligodendrocytes [22], although results are mixed regarding NG2 cells' truly differentiate into astrocytes in vivo [23,24,25]. Additionally, NG2 cell fate mapping rarely labels astrocytes [26,27].

Alongside their ability to respond to injury, NG2 cells also contact neurons under normal conditions and can respond to neurotransmitters. NG2 cells are typically in close proximity of neurons' nodes of Ranvier and synapses on the neuron's somas [28]. Furthermore, these cells can receive input from their synapses with both glutamatergic [29] and GABAergic neurons [30]. NG2 cells can also respond to changes in their membrane potential through their voltage-gated sodium channels [31] and ionotropic glutamate receptors [32].

Attempts to divide neurons into different classes grow more complex as more techniques and characteristics are made available. Initially, Ramón and Cajal classified different neural cells based on their size and morphology, introducing the ideas as projection and interneurons [33]. Since then, it has become possible to identify the neurotransmitters (e.g. GABA) expressed by a neuron, which loosely suggests a neuron's function in the neural circuitry [34]. Attempts to classify specifically GABAergic interneurons have also been based on their different firing patterns [35] and their expression of certain molecular markers; almost all GABAergic interneurons will express one of the following three markers: parvalbumin, which is a calcium-binding protein, somatostatin, a peptide hormone which acts as a neurotransmitter, and 5HT3aR, which is a serotonin receptor [36].

More recently, with the development of RNA sequencing (RNAseq) technologies, new classification efforts have been focused on characterizing the expression of genes that are differentially expressed in closely-related cells that have different physiological properties. Through dimensionality reduction analysis, large data sets with potentially related variables can be simplified while still retaining the most significant components; these reduced data sets can then be graphed to visualize how closely aligned different samples or groups are, based on how similar their components are [37]. Multiple attempts at creating inhibitory interneuron subpopulations based on RNAseq have been performed, with little consensus. One such study claims to establish distinct "cardinal types" of GABAergic interneurons, based on the expression of one of the following molecular markers: parvalbumin, somatostatin, the peptide hormone Vip, the inhibitor of DNA binding gene Id2, the gene that converts tyrosine to dopamine Th, a nitric oxide synthase Nos1, and a binding protein for insulin-like growth factors Igfbp6 [38]. Each of these cardinal types also had associated genes that are more transcribed in that subpopulation;

markers for somatostatin-containing interneurons included a cell membrane glycoprotein Tspan7 and a binding protein for AT-rich sequences Satb1, whereas markers for parvalbumin-containing interneurons included myocyte enhancer factor Mef2c, a receptor tyrosine-kinase Erbb4, and the phospholipase Plcxd3 [38]. Another study using dimension reduction suggests that, even before the actual genes somatostatin or parvalbumin are expressed, there are distinct somatostatin and parvalbumin clusters of embryonic neurons by E14.5 [39]. This study also suggest the cyclin Ccnd2 and zinc-finger transcription factor St18 are early markers of parvalbumin-expressing GABAergic interneurons, whereas the ephedrine receptor Epha5 is a marker for the somatostatin-expressing variety [39]. Although these genes were identified through single cell RNAseq, there have not been attempts at in situ hybridization, immunohistochemistry, or any other experiments to verify these transcripts are being produced or being translated into proteins yet.

Because NG2 cells can react to injuries in vivo, are derived from the same progenitor cell as GABAergic interneurons, and interact with and respond to neurotransmitters, these cells are viable candidates for in vivo reprogramming into neurons after an injury. After a central nervous system injury, introducing either the transcription factor Sox2 alone or both Sox2 and Ascl1 through retroviral vectors was seen to induce NG2 glia to differentiate into neurons expressing doublecortin, a microtubule-associated protein and a marker for immature neurons, in vivo [40]. When a retroviral vector containing the transcription factor NeuroD1 is introduced post-injury, the NG2 cells are reprogrammed into a mix glutamatergic (excitatory) and GABAergic (inhibitory) neurons [41]. With vectors containing Ascl1, Lim homeobox transcription factor Lmx1a, and transcriptionally-inducible nuclear receptor Nurr1 (ALN vectors), more than half of the NG2 glia in the surrounding area are reprogrammed, and the majority of these have the electrophysiological properties of fast-spiking, parvalbumin-containing GABAergic interneurons [42].

Although multiple constructs have been used for transfecting these cells into neurons, using Dlx-2 has been less explored, although its regulatory role in differentiating NPCs suggest this should be a viable construct. Preliminary work done by other members in the Nishiyama lab had looked at trying to induce NPC differentiation into astrocytes, and an RNAseq search looking at differentially expressed transcription factors between NPCs, NG2 cells and astrocytes included Dlx-2. Linda Boshans transfected NG2 cells with a Dlx-2 containing vector (pCMV-Dlx2-IRES2-mCherry) and found that, by 14 days post-transfection (DPT), the transfected NG2 cells had different responses to electrical stimulation in patch-clamp recording experiments than NG2 cells do and they expressed GABA. The majority of these cultures showed immature neuronal characteristics, which include unstable resting potentials, high membrane input resistances, and an inability to produce action potentials [43]; some cultures have fast-spiking characteristics, which are commonly seen in parvalbumin-containing neurons because of their expression of the voltage-gated potassium channels in the KV3 family [44].

Based on these early results, we became interested in the expression of the recently published marker genes for proposed GABAergic interneuron subtypes, hoping to characterize our transfected NG2 cells as mainly expressing markers from either a distinct subtype or multiple

subtypes; because some of the early electrophysiological results included fast-spiking neurons, the early hypothesis was that early parvalbumin marker genes would be some of the most differentially expressed.

To investigate the expression of these characteristic genes, a project focused on quantitative reverse-transcriptase polymerase chain reactions (qRT-PCR) was designed. Using this, the transcription of selected genes of interest can be quantified and compared between different samples, suggesting which proteins are being more expressed. Our transfected NG2 cells are cultured with astrocytes to maintain a healthy cell culture, and we want to ensure that the transfection protocol itself is not driving any changes in expression; to account for these, nearly identical plasmids were created (both were mCherry-containing plasmids, with the only difference being one contained Dlx-2) and transfected into identical cultures. Genes of interest were mainly selected from the two recent papers trying to classify different subpopulations of GABAergic interneurons [38,39], along with three control genes: the OPC cell marker NG2 (which was expected to decrease in expression), the astrocyte marker glial fibrillary acidic protein GFAP, and glutamate decarboxylase 1 (Gad67, the enzyme that produces GABA, which was expected to increase in expression). All samples were collected at 14DPT, to mirror the time point at which the preliminary electrophysiological recordings had taken place.

Materials and Methods

Animals

For all experiments, CD1 mice from Charles River Laboratory (strain #022) were used, and all experiments were approved by the Institutional Animal Care and Use Committee (IACUC).

Cell Culturing (all done by Linda Boshans)

Plasmid Preparation

The entire transcript of mouse Dlx2 cDNA (NM_010054.2, from translation start site to the stop codon) was inserted into a pCMV-IRES2-mCherry vector (obtained from Dr. Hitoshi Gotoh, Kyoto Prefectural Medical University), originally created by adding the mCherry coding sequence in place of the EGFP coding region in a pIRES2-EGFP vector (Clontech).

Purifying, Culturing and Transfecting NG2 Cells

NG2 cells were isolated from the postnatal day 2-3 (P2-3) CD1 mice acquired from the Charles River Laboratory through an adapted version of an established sequential immunopanning purification procedure [45]. Isolated cortices were cut and incubated in a papain solution (20U/ml; Worthington) at 35^{o}C for an hour. Next, these cortices were ground, surrounded by a BSA and ovomucoid solution, and this mixture was passed through a 70-um cell strainer. The ensuing cell suspension was incubated on a petri dish with the O1 antibody (Gift from Dr. Steven Pfeiffer at University of Connecticut Health Center, 1:1 dilution) [46] on its surface to extract the mature oligodendrocytes from the mixture. The remaining supernatant was incubated on another petri dish, which was covered in rat anti-mouse platelet-derived growth factor receptor alpha (PDGFRα) antibody (CD140a, BD Biosciences, 2μg/ml) to isolate the NG2 cells expressing this receptor. The remaining solution was washed away with phosphate-buffered saline (PBS), and the remaining bound NG2 cells were isolated and collected via trypsinization.

These cells were then centrifuged at 1100 rpm for 5 minutes and resuspended in a mixture of platelet-derived growth factor (PDGF) and Dulbecco's Modified Eagle Media containing Sato's supplements (DMEM-Sato's,Peprotech). These cells were then either plated onto glass coverslips (Fisher) with either 100ug/ml of poly-D-lysine (Sigma-Aldrich) and 15 ug laminin (Sigma-Aldrich) or with 30ug/mL of poly-L-lysine (PLL, Sigma-Aldrich) or onto tissue culture dishes (Fischer) also coated with that same concentration of PLL.

16 hours after being plated with the PLL or PDL and laminin, the NG2 cells were transfected with either the pCMV-Dlx2-IRES2-mCherry (Dlx-2) plasmid DNA or the control pCMV-IRES2-mCherry (mCherry) plasmid DNA, using the Lipofectamine 2000 (Invitrogen). Five hours after transfection, the DMEM-Sato's solution with 50ug/mL PDGF-AA (Peprotech) was fully replaced.

Three days post-transfection (DPT), these cells were trypsinized to free them from these plates or coverslips. The freed cells were then plated on an astrocyte-coated glass coverslip

(125,000 astrocytes per 12mm surface area), and a neuronal differentiation media (comprised of 1% N2 supplement [Gibco], 1% B27 [Life Technologies], 1% L-glutamine and 1% Pen-Strep in DMEM/F12 containing 50ng/mL human brain-derived neurotrophic factor [BDNF, Peptrotech]) was applied. This media is again switched at 7DPT to a neuronal maturation media (Neurobasal A supplemented with 2% B27, Glutamax, 1% Pen-Strep and 50 ng/mL human BDNF). Half of the cell culture's media was replaced every three days, and at 10DPT, 1% horse serum was also added to supplement the astrocytes.

Astrocyte Culturing

During the time when NG2 cells were purified, cortical astrocytes were isolated according to previously published protocols [47,48], resuspended in astrocyte media, and placed in a T75 culture flask with the aforementioned 30ug/mL PLL solution, which was changed every 2-3 days. Between days 7 and 9, the astrocyte layer on these flasks covered the entire bottom of the flask, and at this time the flasks were shaken at 260 rpm overnight to free the astrocyte layer from any other cell types. The following day, the free-floating remnants were washed away with PBS. The remaining adhered astrocytes were freed via trypsinization and frozen in aliquots for later plating onto glass coverslips.

qRT-PCR Primer Design

Based on previous GABAergic interneuron subtype analyses, fourteen genes of interest were chosen to be quantified, not including the housekeeping gene Rn7sk. Three of the genes of interest and the housekeeping gene had previously been designed and optimized by researchers in the Nishiyama laboratory. The remaining eleven genes' transcripts were identified on Ensembl [49] and sequences containing exon-exon junctions were selected and used in the NCBI Primer-BLAST tool [50] for primer design. Primers were selected that would produce products between 100 and 200 base pairs long and had low self-complementarity and self 3' complementarity. For the primer sequences, see Table 1.

Table 1

Gene	Forward Primer (bp/Tm in ^{o}C)	Reverse Primer (bp/Tm)
Sst	CCCCAGACTCCGTCAGTTTC (20/60)	GGCTCCAGGGCATCATTCTC (20/61)
Pvalb	GGCCTGAAGAAAAAGAACCCG (21/60)	ATCTTGCCGTCCCCATCCTT (20/61)
Satb1	GTGCGGGATGAACTGAAACG (20/60)	GGCTTCCGGCAACTGTAAGA (20/60)
Mef2c	CACGAGAGCCGGACAAACT (19/60)	AGGTGGAACAGCACACAATCT (21/60)
Ccnd2	TACCTGGACCGTTTCTTGGC (20/60)	CCCAACACTACCAGTTCCCA (20/59)
St18	CAGGGCAAGGACAAAAAGCAC (21/61)	AGCGGGTGGAAAGGTTCAG (19/60)
GFAP*	TGAATCGCTGGAGGAGGAGA (20)	CGTATTGAGTGCGAATCTCTCTCA (24)
Gad67*	ACAGAGACCGACTTCTCCAAC (21)	GAGCGATCAAATGTCTTGCGG (21)

NG2*	CTTCTTCGGGGAGAACCACC (20)	CTTCTGTCCCAGGGCAAGTC (20)
Epha5	TGGAGAGAGACCCTACTGGGA (21/61)	TGATAGAGAGCAGCAGGGCA (20/61)
Vip	TAGCAGAAAATGGCACACCCTA (22/60)	TGTCGTTTGATTGGCACAGG (20/59)
Erbb4	GCTGCTGTTGAACTGGTGTG (20/60)	TCACTAAGACATTGCGGGCT (20/59)
Plcxd3	GCAAACACGACAGACCCAGA (20/61)	TGCATCATGGCGGGAAGAG (19/60)
Id2	GCATCCCACTATCGTCAGCC (20/61)	ATTCGACATAAGCTCAGAAGGGA (23/59)
Rn7sk*	CTCCAAACAAGCTCTCAAGGTCCA (24)	ATGCAGCGCCTCATTTGGATGTGT (24)

Starred genes had been previously designed and optimized by the Nishiyama laboratory

RNA extraction protocol

To prepare the CD1 cortical samples for RNA extraction, the samples first had to be isolated and pulverized. After euthanizing the mouse with carbon dioxide followed by cervical dislocation, Linda removed the brain from the skull, and isolated the cortex from the cerebellum. She then cut the cortex into 100mg parts, flash-froze the samples with liquid nitrogen, and stored them at -80^{o}C. At a later time, I chilled a spatula, mortar and pestle using liquid nitrogen, submerged the piece of cortex in the liquid nitrogen in the mortar, and ground the sample into a fine powder. The sample was then transferred into an Eppendorf tube using the chilled spatula for future steps.

For both the cultured cell samples and the triturated CD1 mouse brain samples, PureLink RNA Mini Kit extraction protocol with DNase was followed according to manufacturer's guidelines [51]. At this point, total RNA had been isolated from the samples and a spectrophotometer was used to test the concentration of the RNA. Finally, 5ug aliquots were made, along with adding 1/10 the volume of TE pH 7.0 to increase stability, and stored at -80^{o}C. To ensure the quality of the samples, all RNA samples used to create cDNA libraries were tested on an Agilent 2200 Tape Station at the Center for Genome Innovation at the University of Connecticut, with the guidance of Bo Reese, who was in charge of sequencing.

cDNA synthesis

The extracted RNA samples underwent cDNA synthesis reactions using the SuperScript IV First-Strand Synthesis System (InVitrogen) according to a modified version of their protocol [52]. Put briefly, between one and two micrograms of RNA was diluted in 10 uL of RNase-free water, 20uM of random hexamers (as opposed to 50uM recommended), and dNTPs to incubate at room temperature. Next, 20uM Oligo(dt)20 was added (as opposed to the 50uM recommended), and the mixture was incubated at 65^{o}C and rapidly placed on ice. Next, a mix of 5x Superscript IV buffer, DTT, RNaseOUT, water and 10 units of Superscript IV (as opposed to 20 units recommended) was added to the RNA mixture and incubated at 50^{o}C for 15 minutes, immediately followed by incubation at 80^{o}C to inactivate the reverse transcriptase, and then placed on ice. Finally, RNase H (New England Biolabs) was added and the tubes were incubated at 37^{o}C to degrade the original RNA. These samples were then diluted to the desired concentration, aliquoted, and stored at -80^{o}C for future use.

Quantifying samples with qPCR

The cDNA produced from a cDNA synthesis reaction with 20 ng of RNA was used for each reaction, mixed with SsoAdvanced Universal SYBR Green Supermix (Bio-Rad, Hercules, CA) as recommended by the manufacturer's protocol for 20uL reactions [53]. The amount of primers added to any given gene's reactions was based on primer optimization experiments (described later in this thesis). Samples were run in duplicate on the Bio-Rad CFX96 (Bio-Rad, Hercules, CA) with the 2 step Amp+Melt protocol. In the amplification portion of the protocol, the first three minutes are at 95^{o}C to activate the transcriptase and denature any double stranded cDNA, followed 40 cycles of ten seconds at 95^{o}C for denaturation, thirty seconds at 55^{o}C for annealing and elongation, and finally a fluorescence measurement to end each cycle to quantify the amount of double stranded DNA product in each well. This is followed by the melting portion of the protocol, which consists of 30 cycles of five seconds at 65^{o}C to allow products to anneal, followed by stepwise 0.5^{o}C increases each second up to 95^{o}C, constantly measuring fluorescence to measure when the products separate. The $2^{-\Delta\Delta CT}$ method was used to determine relative fold changes between samples, with Rn7sk serving as the housekeeping gene for all comparisons.

Results

Primer Optimization

To make sure that all of the genes of interest are adequately expressed in the cDNA library used for primer optimization, mouse P21 cortical tissue was chosen. The expression of Vip, Sst, and Gad21 all are at a maximum by P21, and although PV's expression does not truly peak until P35, there is relatively little change between P21 and P35 [54]. Because of these findings, RNA was isolated from the cortices three different P21 mice, producing five different samples (one from the first mouse and two each from the other two).

To compare the quality of these different RNA samples and determine which is worth using for the primer optimization, a Agilent's Bioanalyzer 2200 Tape Station's High Sensitivity RNA assay was used. This assay uses Agilent's novel RNA Integrity Number (RIN) as a measure for the degradation and quality of an RNA sample, ranging from scores of 1 (completely degraded RNA) to a 10 (intact RNA). This algorithm works with total eukaryotic RNA, taking into account the ratio of the ribosomal 18S and 28S bands and the levels of smaller fragment RNAs compared to those ribosomal bands [55]. Although the initial quality of the RNA can have significant effects on the Ct values for a sample and can slightly affect primer efficiencies; because of this, RIN values above 7.5 (corresponding to minimal degradation and mostly intact RNA) are ideal for any type of qPCR or RNA quantification procedures [56]. The RINs for these five samples ranged from 7.7 to 8.2, with the cortical RNA sample with a RIN of 8.2 being chosen for future cDNA synthesis reactions for qPCR primer optimization (data not shown).

Because a single qPCR plate was used for the optimization and testing of multiple primer pairs, all primers designed here needed similar annealing temperatures. Annealing temperatures are the temperature where the maximum amount of primer is bound to its template, but can vary based on whatever buffers or inhibitors are in the master mix; because of this, a primer's melting temperature is typically predicted by primer design algorithms as a conduit [57]. The melting temperature is the temperature where half of the primers in a solution would be bound to their perfect complement (the template cDNA), so PCR annealing temperatures are typically 4-6 degrees Celsius below the melting temperature of primers. The melting temperature can typically be predicted based on the percentage of guanine and cytosine in the sequence (since these will have 3 hydrogen bonds, compared to the 2 hydrogen bonds between adenine and thymine) and the length of the oligonucleotide primers [58]. Because the qPCR protocol used called for an annealing and elongation step temperature of 55^{o}C, primers were designed to have melting temperatures between 59^{o}C and 61^{o}C, which were attained by keeping GC concentrations between 40% and 60% of the bases in each primer and keeping all primer lengths between 19 and 23 base pairs.

For these designed qPCR primers to meet our lab's standards for quantification, the efficiency of the primers had to be within 5% of 100% efficiency and only amplify a single product. A reaction having 100% efficiency implies that the polymerase enzyme is working at its maximum

capacity (having the same rate of reaction) across each of the different serial dilutions of the cDNA library produced by the cDNA synthesis reaction, and can be calculated by the equation $E = -1+10^{(-1/slope)}$, where the slope refers to the standard curve where the Ct is on the y-axis and the log of the DNA concentration added is on the x-axis [59]. Because the polymerase enzyme working at maximum efficiency will double the amount of the amplicon each cycle, the ΔCt values for each of the five-fold serial dilution is 2.32. During that serial dilution, both the cDNA and any DNA Polymerase inhibitors are being diluted; having less inhibitors in the higher-order serial dilutions than the higher concentration samples can skew the ΔCt values, making them less than this ideal 2.32 and giving an efficiency of over 100%. In higher order dilutions, stochastic effects of how the transcripts are distributed within the volume pipette compared to the rest of the sample can play a larger role as the overall number of transcripts decreases; this means that there can be more variability in Ct values and the ΔCt the more diluted the cDNA samples get [60]. Avoiding changes or introducing any potential inhibitors is a reason why it is important to follow the same RNA isolation protocol exactly when isolating both the RNA for optimization and for the experimental results. Making sure that only the desired section of the gene of interest is being amplified, and no off-target products, is key because the fluorophore in SYBR Green only measures the amount of double-stranded DNA, and not what that DNA segment is. For similar reasons that primers can have different melting temperatures, so can the amplicons; any off-target products produced will most likely have different lengths and different amounts of G-C and A-T bonds, both giving them different melting temperatures and making them separable in a gel electrophoresis; this provided two ways to detect primer non-specificity.

After primer pairs were designed and ordered, multiple genes were optimized on the same qPCR plate. Although the actual amplification curves all overlap (figure 1A), there are distinct melting curve profiles with their own temperature at which maximum dissociation occurred (figure 1B). Looking specifically Id2's amplification, the number of cycles needed for each of the samples in the five-fold serial dilutions to reach threshold was close to the ideal 2.32, but increased slightly as the cDNA was more diluted (figure 1C); as expected, all of the Id2 samples' melt curves have a single peak that align with one another(figure 1D).

For many of the designed primer pairs, the initial primer concentration tested would amplify a single product, but would give an efficiency just outside of that acceptable 95%-105% range (typically within 5-10% of that range). Primers were first tested at a final concentration of 300uM for each of the forward and reverse primer in the qPCR reaction mix, but if this did not give an appropriate reaction efficiency, then primer concentrations of 150uM and 450 uM were both tried as well. All primers used in this study worked at one of these three concentrations.

For the primer pairs targeting Plcxd3 and Erbb4, multiple peaks or more broad curves were generated in their melt curves (figure 2A for Plcxd3), which does not necessarily mean multiple products were generated, but can be an indicator of this. To verify that these primers produced off-target amplicons, the reaction's products were run on a 2% agarose gel alongside a 1Kb Plus DNA Ladder. Multiple bands or smearing in the same well on this gel indicated products of multiple lengths, and therefore multiple products, had been generated (figure 2C for Plcxd3). Another pair of primers for each of these genes was be designed, ordered, and tested; the

second primer pairs for each of these genes met the optimization standards (figure 2B and 2D for Plcxd3).

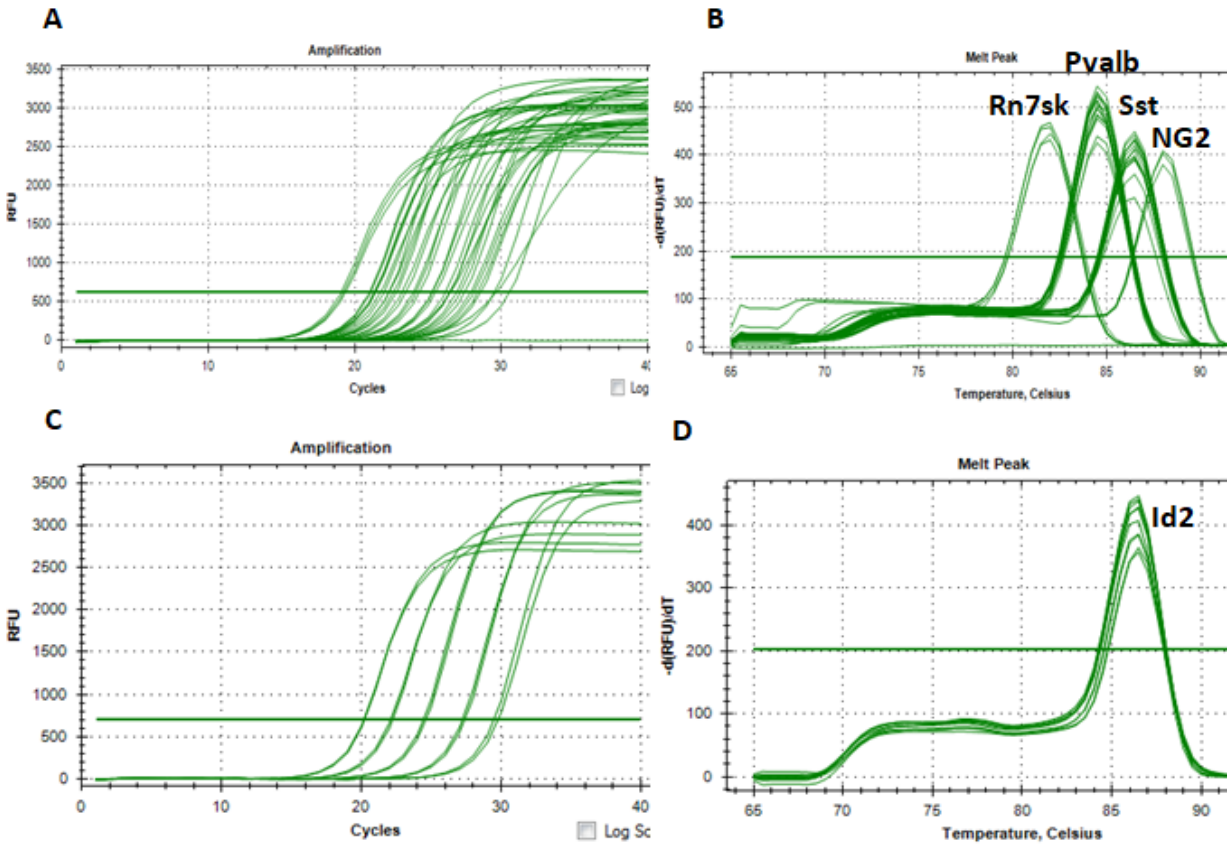

Figure 1: Successful Primer Optimization and Melt Curves

Figure 1. (A) The amplification curves for four different primers show nearly all samples having Ct values between 20 and 30, with the negative control, lacking cDNA, never approaching threshold during the forty cycles. (B). Melt peaks for four different primer sets each have distinct and narrow peaks (from left to right, Rn7sk, Parvalbumin, Somatostatin and NG2), showing specificity of product. These peaks correspond to the temperature at which there was the greatest change in fluorescence, which for SYBR green, indicates when the products went from being double-stranded DNA to single-stranded DNA. (C) The amplification curves for Id2's optimization shows roughly equidistant gaps between the five concentrations of cDNA used [efficiency for these primers were 95.53]. (D) The melt curve and melt peaks for Id2's optimization show each qPCR reaction using the Id2 primers, at the five different cDNA concentrations, all shared the same peak melting temperature and have narrow peaks.

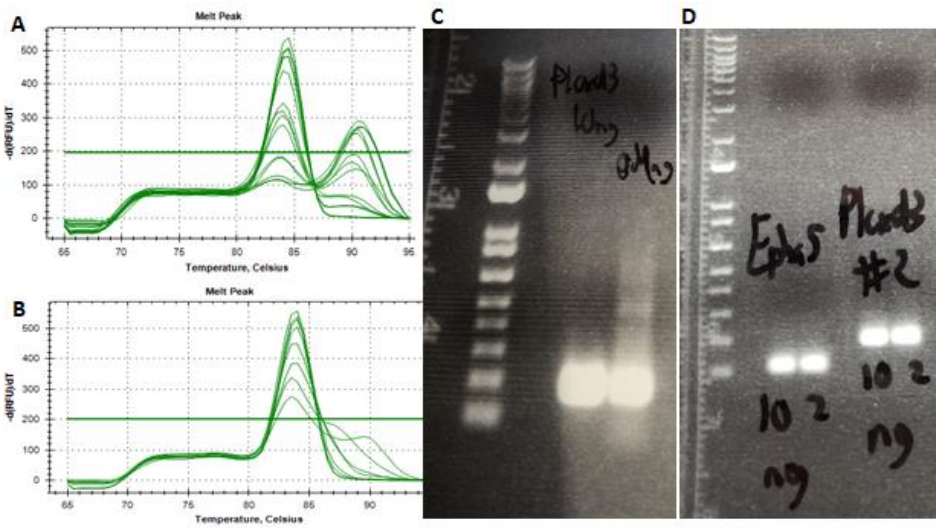

Figure 2: Melt Peaks and Non-Specific Products

Figure 2. The first primer pair designed for the gene Plcxd3 generated a products with multiple melt peaks, implying non-specificity (A). The second primer pair designed for Plcxd3 has a much more consistent peak at approximately 84^{o}C, the same temperature as the largest peak seen when using the previous Plcxd3 primer pair, and less variability outside of the peak (B). When these products were run on 2% agarose gel, The first primer pair's products showed smearing and multiple bands, whereas the second primer pair had one distinct band (C and D).

Transfected NG2 Cell Results

Five replicates of astrocytes, mCherry-transfected NG2 cells, and Dlx2-transfected NG2 cells were cultured and had their RNA extracted. The cDNA generated from each sample in these replicates were used for qPCR, with all samples for the same gene tested on the same qPCR plate at the same time to ensure consistency; all plates were run using the reference gene Rn7sk. For all mCherry-transfected and Dlx2-transfected samples, the housekeeping gene Rn7sk always was within one cycle in terms of reaching threshold for each replicate.

Between the five replicates' qPCR data, the second replicates' comparative Ct (ΔΔCt) values were significantly different across almost every gene. When analyzing the difference in Ct values between each gene of interest and the housekeeping gene for both the experimental Dlx2-transfected samples and the control mCherry-transfected samples (ΔCtE and ΔCtC, respectively), there were no noticeable outliers compared to the rest of the replicates. However, the difference between the ΔCtE and ΔCtC (ΔΔCt) does stand out for these samples: in replicate #2, every gene except Gad67 and Vip appears to have reduced expression in the Dlx2-transfected sample, whereas in the average of the other 4 replicates, every gene except for Id2 appears to be transcribed at higher levels in the Dlx2-transfected samples (data not shown). Because the supermajority of genes have the opposite expression fold changes in this one replicate, it has been excluded from all future analysis.

The relative expression fold changes of the four analyzed replicates show that marker genes from multiple subtypes are differentially expressed in the Dlx2-transfected samples (Figure 3).

Gad67 is significantly more transcribed in these samples, indicating that the transfected NG2 cells are more able to produce GABA and are likely transforming into inhibitory neurons. Although not statistically significantly altered because of relatively large standard deviation, Id2's average expression rate has decreased in this sample, indicating these newly-forming GABAergic interneurons are probably not belonging to this cardinal subtype. However, one marker gene for each of somatostatin- and parvalbumin-subtype (Satb1 and Erbb4, respectively) interneurons, along with somatostatin itself, are significantly more transcribed in the Dlx2-transfected population; the cardinal subtype gene Vip also has increased expression in all four replicates, hinting at a mixed phenotype.

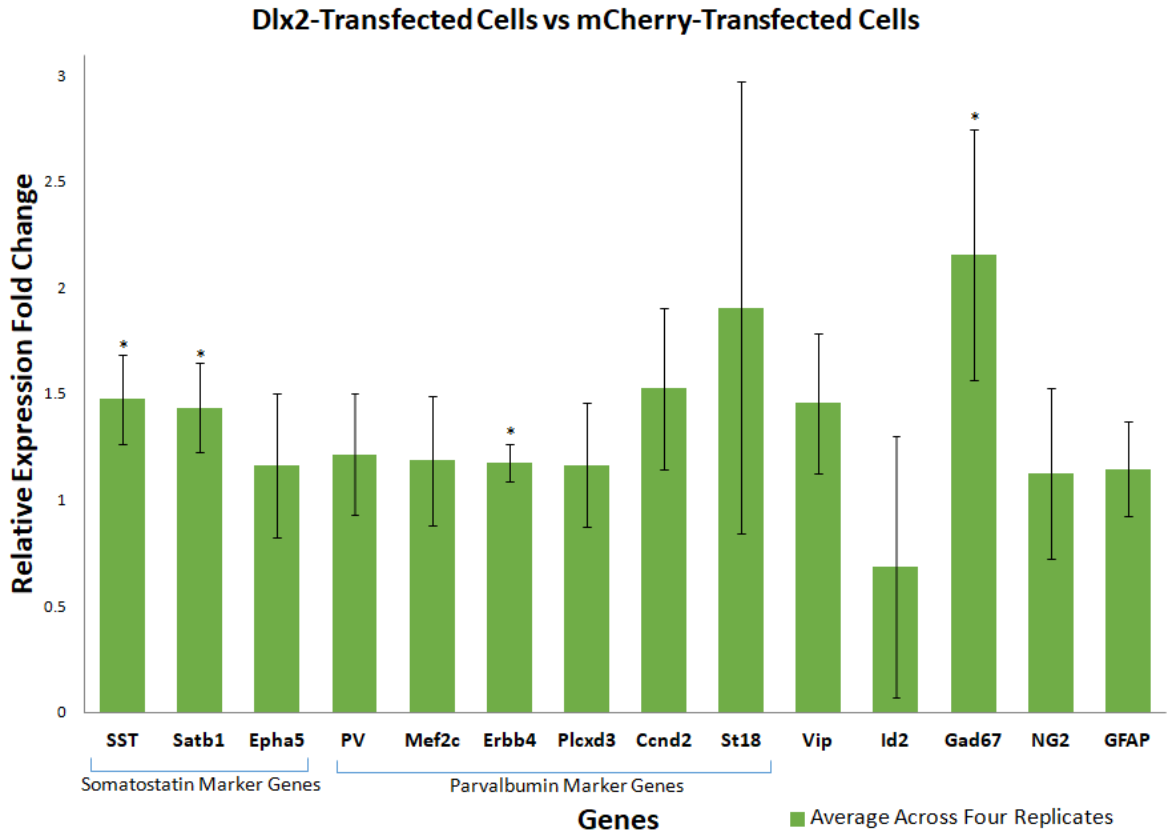

Figure 3: qPCR Expression Changes in Transfected NG2 Samples

Figure 3. The relative expression fold changes of the genes of interest between the NG2 cells transfected with the Dlx2-vector and the mCherry-vector. Many of the marker genes for somatostatin- and parvalbumin-expressing GABAergic interneurons are more transcribed in the Dlx2-transfected cells. Somatostatin, its marker gene Satb1, the Parvalbumin marker gene Erbb4, and the GABA-producing Gad67 gene are all significantly differentially expressed ($p<0.05$) according to a student's t-test for these samples.

Because each of these replicates was cultured and stored at separate times before RNA extraction, and each sample's RNA extraction was run in parallel, there could have been differences in the quality of RNA derived from each sample. All samples from replicates one through four had at least a RIN of 7.9, with almost all samples with RIN values in the 8s (data not shown). However, replicate 5 had significantly worse RIN values, with the Dlx2-transfected

sample having a RIN of 7.1, and the mCherry-transfected sample having a RIN of 6.8 (data not shown). Because these values are below the general standards for intact RNA, replicate 5's qPCR data can also be reasonably excluded from future analysis.

Excluding replicate five from relative expression analysis shows that most genes of interest appear to be similarly expressed in the remaining samples, but moving from n=4 to n=3 can negatively affect the statistical significance (Figure 4). There are two genes (somatostatin marker Satb1 and early parvalbumin marker Ccnd2) in which replicate 5 had been an outlier, and removing replicate five increased the statistical significance of their expression fold change to below ($p<0.01$) by greatly decreasing the standard deviations. The actual replicate 5 comparative Ct for Erbb4 lined up with the other replicates, and losing that sample increased the standard deviation enough to no longer make that gene's change in expression statistically significant. In spite of removing replicate 5, the data still suggests a mixed GABAergic phenotype for these Dlx2-transfected cells.

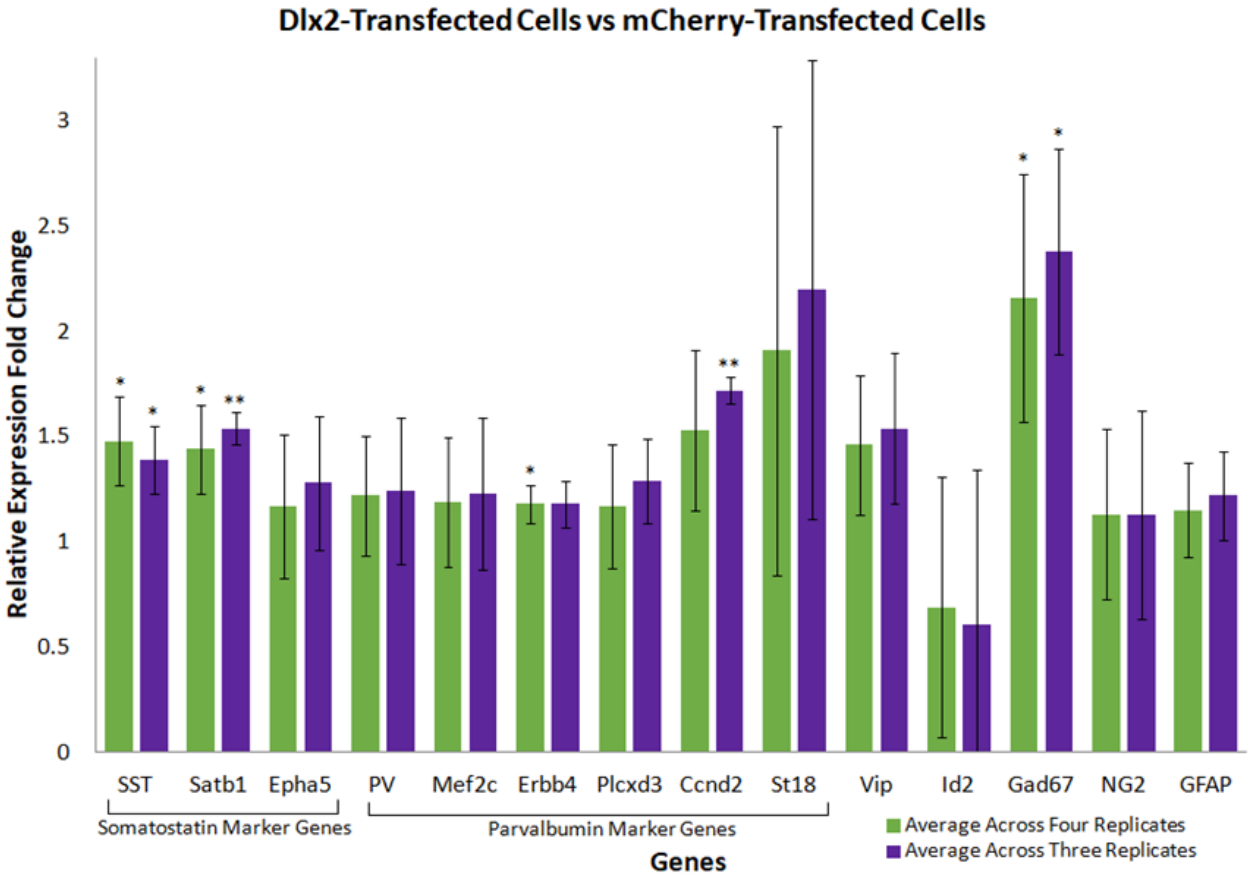

Figure 4: qPCR Expression Changes Comparison when Excluding Low-Quality Samples
Figure 4 After excluding replicate 5 due to poor RIN values for its RNA, there changes in average expression fold change are relatively minor. A student's t-test (* indicates $p<0.05$, ** indicates $p<0.01$) shows that statistical significance was lost for the parvalbumin marker gen Erbb4 by removing replicate 5, but early parvalbumin marker gene Ccnd2 and somatostatin marker Satb1 both gained in statistical significance.

The raw Ct values for this data also gives an idea of how expressed these genes of interest are in our samples. Because primers with efficiencies of 100 ± 5% were chosen, the amount of transcript should double in each qPCR cycle. Genes that are more expressed need less cycles to reach their Ct value. Ct values are most reliable within their linear dynamic range of 20 and 30 [61], and Ct values above 35 will have more variability, making them less reliable for analysis [62]. All of the average Ct values fell between 20 and 35 with the exception of GFAP, which is only highly expressed in the astrocytes these NG2 cells were plated onto.

The Ct values for the Dlx2-transfected samples put into perspective the significant increase in transcription of certain genes. Somatostatin's Ct value average among samples is 34, whereas parvalbumin's average Ct value is 23. This means that, although the transcription of somatostatin was significantly increased in the Dlx2-transfected sample, there was still

approximately a 2000-fold expression difference between somatostatin and parvalbumin, suggesting parvalbumin may be influencing the phenotype of these GABAergic interneurons more than previous analysis suggested. Along similar lines, although Vip is transcribed at higher levels in the Dlx-transfected samples in figures 3 and 4, its average Ct value is only 31, leaving it 250 times less expressed than parvalbumin in these samples (although more expressed than somatostatin). For reference, the somatostatin marker genes and all of the parvalbumin marker genes except Plcxd3 have average Ct values between 21 and 26, suggesting somatostatin's expression could continue to increase to approach these Ct values if a later time point were tested (data not shown).

Discussion

Although the advent of RNA sequencing has given much more information on which genes are expressed in specific cells, how to best use this data is still unclear. Past classifications of neurons have all been based on easily observable or more clearly defined characteristics (their electrophysiology, morphology, which neurotransmitters and receptors they express, etc., (DeFelipe 2013)); it is not as easy to determine how a particular gene being more or less expressed can affect a cell's functions, especially when many genes' expressions are correlated, like the genes listed as markers for Mi's and Mayer's cardinal types of neurons. There is currently no standard for what level of difference would be needed in the gene expression between groups of cells to classify them as different groups, or if these different groups would even have different functions within the central nervous system.

Dimensionality reduction techniques have provided a statistical way to try and cope with these issues with large data sets, but still have their own issues. Feature selection approaches, where discrete pieces of data (for example, the expression of one intentionally selected gene) are compared directly, can be too difficult to parse or find meaning in when tens, hundreds or thousands of features could be selected; dimensionality reduction tries to approach this problem by finding which components (or eigenvectors) are the most significant (or has the highest eigenvalue) when finding differences between groups, and can transform this data graphically to highlight differences. Some techniques, like linear discriminant analysis (LDA) and t-distributed stochastic neighbor embedding (t-SNE), are considered "supervised" and are meant to maximize differences between groups when samples have already been arbitrarily put into groups; unsupervised techniques like principal component analysis (PCA, which is used in both the Meyer et al. 2018 and Mi et al. 2018 studies) are meant to maximize variance between each sample, and any type of grouping can be done after the fact [63]. Some methods, like PCA, rely on linear algebra and will produce the same result every time they are performed on the same data set; other methods, like t-SNE and LDA, can provide "less stable" results, giving slightly different results in different iterations performed with the same data [64]. Because of these differences, it is understandable why these preliminary studies are using PCA; once there is more consensus on what groups or subgroups of GABAergic interneurons exist, techniques like LDA may be more informative.

The optimization process for these qPCR primers relied upon two different parameters: amplifying a single product, and operating within 5% of 100% primer efficiency. During primer design with Primer-BLAST, primers were already run through a computer algorithm to look for potential off-target products that could be amplified in the mouse genome, but it is still important to verify that only a single product is being generated by the primers. Because the melting point of any amplicon depends on both the length of the amplicon and the actual sequence's amounts of C-G and A-T bonds, melting points of amplicons are an easy way to screen for multiple, different amplicons being produced. Having a narrow, sharp melting curve peak indicates that all of these amplicons are dissociating with their complementary strand at the same temperature; because that dissociation depends on the composition of the bonds and how many there are, this is a reasonable conduit for looking at product specificity. When multiple peaks

were seen in two of the primer pairs tested, this suggested that either amplicons of different lengths or amplicons with different nucleotide compositions had been generated, and the gel electrophoresis confirmed both times that products of different lengths had been amplified. This was a clear sign that the primer pairs in question were not amplifying a single, specific product, and prompted the ordering of new primer pairs. Because the effects of primer and reaction inefficiency are compounded each cycle, it was imperative that these reactions are optimized before being used in experiments, or else Ct values could vary significantly. The ΔΔCt method relies upon the quantification of the cDNA of a particular gene in two different groups of samples (here, iterations of both the Dlx-2-transfected samples and the mCherry-transfected samples), so if any of those samples differ in the starting amount of of cDNA of that particular gene, the unoptimized reaction's compounding error would skew the results and any comparisons made between samples.

Although parvalbumin is much more expressed in these transfected samples than somatostatin is, the parvalbumin expression is also quite high and variable in even the astrocyte-only samples from the replicates, with a Ct range between 23 and 29 (data not shown). There is a chance the way the cell culture itself was designed is leading to high parvalbumin expression, and not the NG2 cells being transfected; the lack of statistical significance in the change of expression of parvalbumin in the analysis would support this. Finding a way to prepare and transfect the NG2 cells using less or no astrocytes could reduce this level of background noise and make better comparisons of parvalbumin and somatostatin expression levels in the qPCR samples possible.

Our research confirms that transfecting NG2 cells with a Dlx2-vector increases the expression of some genes required for becoming inhibitory GABAergic interneurons by 14DPT, including the GABA-producing Gad67 and various somatostatin and parvalbumin marker genes. The variety of classes of marker genes having increased expression, and the lack of all genes in any given category being differentially expressed) suggests a mixed phenotype, but further electrophysiological testing or gene expression analysis at a time point later than 14DPT could strengthen this characterization, since different GABAergic interneuron types have different characteristic responses [42]. Confirming the expression of key genes, like Gad67, parvalbumin, somatostatin and Vip through in situ hybridization can also be useful in classifying this type.

Although we have shown increases in key GABAergic interneuron genes by 14DPT, future experiments looking at 2DPT and 7DPT could shed further light onto which genes' transcription levels are first affected, and could potentially lead to finding the mechanism of how increasing Dlx2 can cause this transformation in NG2 cells. Increasing the number of replicates tested could also help reduce the standard deviations and better elucidate which genes' expressions are significantly affected, rather than just being affected as an outlier in one or two replicates enough to skew the data.

Conclusion

Recent studies have shown NG2 cells can be transformed to follow a neuronal fate, and which of the constructs were used affect what types of neurons are produced. Recent attempts on how to classify different types of GABAergic interneurons lacks consensus, so for this study, genes of interest were identified from multiple studies. Overall, fourteen novel primer pairs for qRT-PCR were used and optimized for providing insight into what types of neurons are produced by our Dlx-2-transfected NG2 cells. Electrophysiological testing at 14DPT mainly showed an immature GABAergic neuronal phenotype for these cells, with a minority behaving more like fast-spiking parvalbumin-containing GABAergic interneurons. The qRT-PCR results from 14DPT samples also show that the GABA-producing Gad67 is significantly more expressed, alongside a few parvalbumin- and somatostatin-subtype associated genes, but most genes are not significantly changed in their expression, suggesting a mixed phenotype for these Dlx-2-transfected cells, at least at this time point.

Acknowledgements

I would like to thank Dr. Akiko Nishiyama for providing me the materials, training and guidance necessary for completing this project aiding with interpreting the data. I would also like to thank graduate students in the Nishiyama lab Amin Sherafat and Linda Boshans for training me, and Linda Boshans specifically for doing the cell culture portion of this project and encouraging me during the most trying parts of this project. Thanks also go to the University of Connecticut for providing me this opportunity.

References

1. Buffo, Annalisa, et al. “Expression Pattern of the Transcription Factor Olig2 in Response to Brain Injuries: Implications for Neuronal Repair.” PNAS, National Academy of Sciences, 13 Dec. 2005, www.pnas.org/content/102/50/18183.short.
2. Robel, Stefanie, et al. “The Stem Cell Potential of Glia: Lessons from Reactive Gliosis.” Nature Reviews Neuroscience, vol. 12, no. 2, 2011, pp. 88–104., doi:10.1038/nrn2978. https://www.nature.com/articles/nrn2978
3. Sofroniew, Michael V. “Molecular Dissection of Reactive Astrogliosis and Glial Scar Formation.” Trends in Neurosciences, vol. 32, no. 12, 2009, pp. 638–647., doi:10.1016/j.tins.2009.08.002. https://www.ncbi.nlm.nih.gov/pmc/articles/PMC2787735/
4. Peters, Alan. “A Fourth Type of Neuroglial Cell in the Adult Central Nervous System.” Journal of Neurocytology, vol. 33, no. 3, 2004, pp. 345–357., doi:10.1023/b:neur.0000044195.64009.27. https://www.ncbi.nlm.nih.gov/pubmed/15475689/
5. Zhu, X., et al. “NG2 Cells Generate Both Oligodendrocytes and Gray Matter Astrocytes.” Development, vol. 135, no. 1, 2007, pp. 145–157., doi:10.1242/dev.004895. https://www.ncbi.nlm.nih.gov/pubmed/18045844
6. Nishiyama, Akiko, et al. “NG2 Glial Cells: A Novel Glial Cell Population in the Adult Brain.” Journal of Neuropathology and Experimental Neurology, vol. 58, no. 11, 1999, pp. 1113–1124., doi:10.1097/00005072-199911000-00001. https://www.ncbi.nlm.nih.gov/pubmed/10560654
7. Nishiyama, Akiko, et al. “Polydendrocytes (NG2 Cells): Multifunctional Cells with Lineage Plasticity.” Nature Reviews Neuroscience, vol. 10, no. 1, 2009, pp. 9–22., doi:10.1038/nrn2495. https://www.ncbi.nlm.nih.gov/pubmed/19096367/
8. Trotter, Jacqueline, et al. “NG2 Cells: Properties, Progeny and Origin.” Brain Research Reviews, vol. 63, no. 1-2, 2010, pp. 72–82., doi:10.1016/j.brainresrev.2009.12.006. https://www.ncbi.nlm.nih.gov/pmc/articles/PMC2862831/
9. Binamé, Fabien. “Transduction of Extracellular Cues into Cell Polarity: the Role of the Transmembrane Proteoglycan NG2.” Molecular Neurobiology, vol. 50, no. 2, 2014, pp. 482–493., doi:10.1007/s12035-013-8610-8. https://link.springer.com/article/10.1007%2Fs12035-013-8610-8
10. Kessaris, Nicoletta, et al. “Specification of CNS Glia from Neural Stem Cells in the Embryonic Neuroepithelium.” Philosophical Transactions of the Royal Society of London. Series B, Biological Sciences, The Royal Society, 12 Jan. 2008, www.ncbi.nlm.nih.gov/pmc/articles/PMC2605487/. https://www.ncbi.nlm.nih.gov/pmc/articles/PMC2605487/
11. Juarez, Alejandro Lopez, et al. “Oligodendrocyte Progenitor Programming and Reprogramming: Toward Myelin Regeneration.” Brain Research, vol. 1638, 2016, pp. 209–220., doi:10.1016/j.brainres.2015.10.051. https://www.ncbi.nlm.nih.gov/pmc/articles/PMC5119932/
12. Pringle, N.P., et al. “PDGF Receptors in the Rat CNS: during Late Neurogenesis, PDGF Alpha-Receptor Expression Appears to Be Restricted to Glial Cells of the Oligodendrocyte Lineage.” Development, The Company of Biologists Ltd, 1 June 1992,

dev.biologists.org/content/115/2/535.long. http://dev.biologists.org/cgi/pmidlookup?view=long&pmid=1425339
13. Nishiyama, A., et al. “Co-Localization of NG2 Proteoglycan and PDGF A-Receptor on O2A Progenitor Cells in the Developing Rat Brain.” Journal of Neuroscience Research, vol. 43, no. 3, 1996, pp. 299–314., doi:10.1002/(sici)1097-4547(19960201)43:3<299::aid-jnr5>3.0.co;2-e. https://onlinelibrary.wiley.com/doi/abs/10.1002/%28SICI%291097-4547%2819960201%2943%3A3%3C299%3A%3AAID-JNR5%3E3.0.CO%3B2-E
14. Gotoh, Hitoshi, et al. “NG2 Expression in NG2 Glia Is Regulated by Binding of SoxE and BHLH Transcription Factors to a Cspg4 Intronic Enhancer.” Glia, vol. 66, no. 12, 2018, pp. 2684–2699., doi:10.1002/glia.23521. https://onlinelibrary.wiley.com/doi/full/10.1002/glia.23521
15. He, Wenlei, et al. “Multipotent Stem Cells from the Mouse Basal Forebrain Contribute GABAergic Neurons and Oligodendrocytes to the Cerebral Cortex during Embryogenesis.” The Journal of Neuroscience, vol. 21, no. 22, 2001, pp. 8854–8862., doi:10.1523/jneurosci.21-22-08854.2001. http://www.jneurosci.org/content/21/22/8854.long
16. Petryniak, Magdalena A., et al. “Dlx1 And Dlx2 Control Neuronal versus Oligodendroglial Cell Fate Acquisition in the Developing Forebrain.” Neuron, vol. 55, no. 3, 2007, pp. 417–433., doi:10.1016/j.neuron.2007.06.036. https://www.ncbi.nlm.nih.gov/pmc/articles/PMC2039927/
17. Paina, S., et al. “Wnt5a Is a Transcriptional Target of Dlx Homeogenes and Promotes Differentiation of Interneuron Progenitors In Vitro and In Vivo.” Journal of Neuroscience, vol. 31, no. 7, 2011, pp. 2675–2687., doi:10.1523/jneurosci.3110-10.2011. https://www.ncbi.nlm.nih.gov/pubmed/21325536
18. Berghoff, E. G., et al. “Evf2 (Dlx6as) LncRNA Regulates Ultraconserved Enhancer Methylation and the Differential Transcriptional Control of Adjacent Genes.” Development, vol. 140, no. 21, 2013, pp. 4407–4416., doi:10.1242/dev.099390. https://www.ncbi.nlm.nih.gov/pmc/articles/PMC4007716/
19. Anderson, Stewart A, et al. “Mutations of the Homeobox Genes Dlx-1 and Dlx-2 Disrupt the Striatal Subventricular Zone and Differentiation of Late Born Striatal Neurons.” Neuron, vol. 19, no. 1, 1997, pp. 27–37., doi:10.1016/s0896-6273(00)80345-1. https://www.ncbi.nlm.nih.gov/pubmed/9247261/
20. Poitras, L., et al. “An SNP in an Ultraconserved Regulatory Element Affects Dlx5/Dlx6 Regulation in the Forebrain.” Development, vol. 137, no. 18, 2010, pp. 3089–3097., doi:10.1242/dev.051052. https://www.ncbi.nlm.nih.gov/pubmed/20702565
21. Kondo, T., and M. Raff. “Oligodendrocyte Precursor Cells Reprogrammed to Become Multipotential CNS Stem Cells.” Science, vol. 289, no. 5485, 2000, pp. 1754–1757., doi:10.1126/science.289.5485.1754. https://www.ncbi.nlm.nih.gov/pubmed/10976069/
22. Hackett, Amber R., and Jae K. Lee. “Understanding the NG2 Glial Scar after Spinal Cord Injury.” Frontiers in Neurology, vol. 7, 2016, doi:10.3389/fneur.2016.00199. https://www.ncbi.nlm.nih.gov/pmc/articles/PMC5108923/
23. Alonso, G. “NG2 Proteoglycan-Expressing Cells of the Adult Rat Brain: Possible Involvement in the Formation of Glial Scar Astrocytes Following Stab Wound.” Glia, vol.

49, no. 3, 2004, pp. 318–338., doi:10.1002/glia.20121. https://onlinelibrary.wiley.com/doi/full/10.1002/glia.20121
24. Komitova, Mila, et al. “NG2 Cells Are Not a Major Source of Reactive Astrocytes after Neocortical Stab Wound Injury.” Glia, vol. 59, no. 5, 2011, pp. 800–809., doi:10.1002/glia.21152. https://www.ncbi.nlm.nih.gov/pmc/articles/PMC3560299/
25. Dimou, L., et al. “Progeny of Olig2-Expressing Progenitors in the Gray and White Matter of the Adult Mouse Cerebral Cortex.” Journal of Neuroscience, vol. 28, no. 41, 2008, pp. 10434–10442., doi:10.1523/jneurosci.2831-08.2008. http://www.jneurosci.org/content/28/41/10434.long
26. Rivers, Leanne E, et al. “PDGFRA/NG2 Glia Generate Myelinating Oligodendrocytes and Piriform Projection Neurons in Adult Mice.” Nature Neuroscience, vol. 11, no. 12, 2008, pp. 1392–1401., doi:10.1038/nn.2220. https://www.ncbi.nlm.nih.gov/pmc/articles/PMC3842596/
27. Zhu, X., et al. “NG2 Cells Generate Both Oligodendrocytes and Gray Matter Astrocytes.” Development, vol. 135, no. 1, 2007, pp. 145–157., doi:10.1242/dev.004895. http://dev.biologists.org/content/135/1/145.long
28. Wigley, Rebekah, and Arthur M. Butt. “Integration of NG2-Glia (Synantocytes) into the Neuroglial Network.” Neuron Glia Biology, vol. 5, no. 1-2, 2009, p. 21., doi:10.1017/s1740925x09990329. https://www.ncbi.nlm.nih.gov/pubmed/19785922/
29. Bergles, Dwight E., et al. “Glutamatergic Synapses on Oligodendrocyte Precursor Cells in the Hippocampus.” Nature, vol. 405, no. 6783, 2000, pp. 187–191., doi:10.1038/35012083. https://www.ncbi.nlm.nih.gov/pubmed/10821275/
30. Paukert, Martin, and Dwight E Bergles. “Synaptic Communication between Neurons and NG2 Cells.” Current Opinion in Neurobiology, vol. 16, no. 5, 2006, pp. 515–521., doi:10.1016/j.conb.2006.08.009. https://www.ncbi.nlm.nih.gov/pubmed/16962768
31. Káradóttir, Ragnhildur, et al. “Spiking and Nonspiking Classes of Oligodendrocyte Precursor Glia in CNS White Matter.” Nature Neuroscience, U.S. National Library of Medicine, Apr. 2008, www.ncbi.nlm.nih.gov/pubmed/18311136/. https://www.ncbi.nlm.nih.gov/pubmed/18311136/
32. De Biase, Lindsay M, et al. “Excitability and Synaptic Communication within the Oligodendrocyte Lineage.” The Journal of Neuroscience : the Official Journal of the Society for Neuroscience, U.S. National Library of Medicine, 10 Mar. 2010, www.ncbi.nlm.nih.gov/pmc/articles/PMC2838193/. https://www.ncbi.nlm.nih.gov/pmc/articles/PMC2838193/
33. Ramón y Cajal S. (1911). *Histologie du Système Nerveux de L’homme & des Vertébrés*, Vol. II Paris: Maloine.
34. DeFelipe, Javier et al. “New Insights into Cortical Interneurons Development and Classification: Contribution of Developmental Studies.” Developmental Neurobiology, vol. 71, no. 1, 2010, pp. 34–44., doi:10.1002/dneu.20810. https://www.ncbi.nlm.nih.gov/pmc/articles/PMC3619199/
35. “Petilla Terminology: Nomenclature of Features of GABAergic Interneurons of the Cerebral Cortex.” Nature Reviews Neuroscience, vol. 9, no. 7, 2008, pp. 557–568., doi:10.1038/nrn2402. https://www.ncbi.nlm.nih.gov/pmc/articles/PMC2868386/

36. Rudy, Bernardo, et al. “Three Groups of Interneurons Account for Nearly 100% of Neocortical GABAergic Neurons.” Developmental Neurobiology, vol. 71, no. 1, 2010, pp. 45–61., doi:10.1002/dneu.20853. https://www.ncbi.nlm.nih.gov/pubmed/21154909?dopt=Abstract
37. Ray, Sunil, and Business Analytics. “Beginners Guide To Learn Dimension Reduction Techniques.” Analytics Vidhya, 19 Oct. 2015, www.analyticsvidhya.com/blog/2015/07/dimension-reduction-methods/.
38. Mayer, Christian, et al. “Developmental Diversification of Cortical Inhibitory Interneurons.” Nature News, Nature Publishing Group, 5 Mar. 2018, www.nature.com/articles/nature25999.
39. Mi, Da, et al. “Early Emergence of Cortical Interneuron Diversity in the Mouse Embryo.” Science, vol. 360, no. 6384, 2018, pp. 81–85., doi:10.1126/science.aar6821. http://science.sciencemag.org/content/360/6384/81.long
40. Heinrich, Christophe, et al. “Sox2-Mediated Conversion of NG2 Glia into Induced Neurons in the Injured Adult Cerebral Cortex.” Stem Cell Reports, vol. 3, no. 6, 2014, pp. 1000–1014., doi:10.1016/j.stemcr.2014.10.007. https://www.sciencedirect.com/science/article/pii/S2213671114003294
41. Guo, Ziyuan, et al. “In Vivo Direct Reprogramming of Reactive Glial Cells into Functional Neurons after Brain Injury and in an Alzheimer’s Disease Model.” Cell Stem Cell, vol. 14, no. 2, 2014, pp. 188–202., doi:10.1016/j.stem.2013.12.001. https://www.ncbi.nlm.nih.gov/pubmed/24360883
42. Pereira, Maria, et al. “Direct Reprogramming of Resident NG2 Glia into Neurons with Properties of Fast-Spiking Parvalbumin-Containing Interneurons.” Stem Cell Reports, vol. 9, no. 3, 2017, pp. 742–751., doi:10.1016/j.stemcr.2017.07.023. https://www.ncbi.nlm.nih.gov/pmc/articles/PMC5599255/
43. Magnuson, David S.k., et al. “In Vivo Electrophysiological Maturation of Neurons Derived from a Multipotent Precursor (Embryonal Carcinoma) Cell Line.” Developmental Brain Research, vol. 84, no. 1, 1995, pp. 130–141., doi:10.1016/0165-3806(94)00166-w. https://www.sciencedirect.com/science/article/pii/016538069400166W?via%3Dihub
44. Freund, Tamas, and Szabolcs Kali. “Interneurons.” Scholarpedia, Brain Corporation, 2008, www.scholarpedia.org/article/Interneurons. http://www.scholarpedia.org/article/Interneurons
45. Emery, Ben, and Jason C. Dugas. “Purification of Oligodendrocyte Lineage Cells from Mouse Cortices by Immunopanning.” Cold Spring Harbor Protocols, vol. 2013, no. 9, 2013, doi:10.1101/pdb.prot073973. http://cshprotocols.cshlp.org/content/2013/9/pdb.prot073973.long
46. Sommer, I., and M. Schachner. “Monoclonal Antibodies (O1 to O4) to Oligodendrocyte Cell Surfaces: An Immunocytological Study in the Central Nervous System.” Developmental Biology, vol. 83, no. 2, 1981, pp. 311–327., doi:10.1016/0012-1606(81)90477-2. https://www.ncbi.nlm.nih.gov/pubmed/6786942
47. Kaech, Stefanie, and Gary Banker. “Culturing Hippocampal Neurons.” Nature Protocols, vol. 1, no. 5, 2006, pp. 2406–2415., doi:10.1038/nprot.2006.356. https://www.ncbi.nlm.nih.gov/pubmed/17406484

48. Schildge, Sebastian, et al. “Isolation and Culture of Mouse Cortical Astrocytes.” Journal of Visualized Experiments, no. 71, 2013, doi:10.3791/50079. https://www.ncbi.nlm.nih.gov/pubmed/?term=Schildge+2013
49. “Ensembl Release 94.” Ensembl, US East, Oct. 2018, useast.ensembl.org/index.html
50. *Primer-BLAST: A Tool for Finding Specific Primers.* U.S. National Library of Medicine, 2018, www.ncbi.nlm.nih.gov/tools/primer-blast/.
51. PureLink RNA Mini Kit User Guide. Ambion by Life Technologies, 14 June 2012, assets.thermofisher.com/TFS-Assets/LSG/manuals/purelink_rna_mini_kit_man.pdf.
52. SuperScript IV Reverse Transcriptase User Guide. Life Technologies, 3 Feb. 2015, tools.thermofisher.com/content/sfs/manuals/SSIV_Reverse_Transcriptase_UG.pdf.
53. SsoAdvanced Universal SYBR Green Supermix. Bio-Rad, 2013, www.bio-rad.com/webroot/web/pdf/lsr/literature/10031339.pdf.
54. Ueda, Shuhei, et al. “Sequence of Molecular Events during the Maturation of the Developing Mouse Prefrontal Cortex.” Molecular Neuropsychiatry, vol. 1, no. 2, 2015, pp. 94–104., doi:10.1159/000430095. https://www.ncbi.nlm.nih.gov/pmc/articles/PMC4596535/
55. Mueller, Odilo, et al. RNA Integrity Number (RIN) - Standardization of RNA Quality Control. Agilent, 21 Jan. 2016, www.agilent.com/cs/library/applications/5989-1165EN.pdf.
56. Fleige, Simone, et al. “Comparison of Relative MRNA Quantification Models and the Impact of RNA Integrity in Quantitative Real-Time RT-PCR.” Biotechnology Letters, vol. 28, no. 19, 2006, pp. 1601–1613., doi:10.1007/s10529-006-9127-2. https://www.ncbi.nlm.nih.gov/pubmed/?term=Huch+Fleige
57. Bustin, Stephen, and Jim Huggett. “QPCR Primer Design Revisited.” Biomolecular Detection and Quantification, vol. 14, 2017, pp. 19–28., doi:10.1016/j.bdq.2017.11.001. https://www.ncbi.nlm.nih.gov/pmc/articles/PMC5702850/
58. Santalucia, J. “A Unified View of Polymer, Dumbbell, and Oligonucleotide DNA Nearest-Neighbor Thermodynamics.” Proceedings of the National Academy of Sciences, vol. 95, no. 4, 1998, pp. 1460–1465., doi:10.1073/pnas.95.4.1460. https://www.ncbi.nlm.nih.gov/pmc/articles/PMC19045/
59. “QPCR Efficiency Calculator.” Thermo Fisher Scientific - US, www.thermofisher.com/us/en/home/brands/thermo-scientific/molecular-biology/molecular-biology-learning-center/molecular-biology-resource-library/thermo-scientific-web-tools/qpcr-efficiency-calculator.html.
60. Cepin, Urska. “Understanding QPCR Efficiency and Why It Exceeds 100%.” Biosistemika, 26 Apr. 2018, biosistemika.com/blog/qpcr-efficiency-over-100/.
61. Kuang, Jujiao, et al. “An Overview of Technical Considerations When Using Quantitative Real-Time PCR Analysis of Gene Expression in Human Exercise Research.” Plos One, vol. 13, no. 5, 2018, doi:10.1371/journal.pone.0196438. https://www.ncbi.nlm.nih.gov/pmc/articles/PMC5944930/
62. Nolan, Tania, et al. “Quantification of MRNA Using Real-Time RT-PCR.” Nature News, Nature Publishing Group, 9 Nov. 2006, www.nature.com/articles/nprot.2006.236. https://www.nature.com/articles/nprot.2006.236

63. Raschka, Sebastian. Linear Discriminant Analysis. 3 Aug. 2014, https://sebastianraschka.com/Articles/2014_python_lda.html#principal-component-analysis-vs-linear-discriminant-analysis.
64. Cohen, Elior. “Reducing Dimensionality from Dimensionality Reduction Techniques.” Towards Data Science, 2 July 2017, https://towardsdatascience.com/reducing-dimensionality-from-dimensionality-reduction-techniques-f658aec24dfe.